ACOUSTIC ANALYSIS OF MRI SCANNERS

W. Shao and C. K. Mechefske
Department of Mechanical and Materials Engineering, Queen's University,
Kingston, Ontario, Canada K7L 3N6 Email: shao@me.queensu.ca

1. INTRODUCTION

Acoustic noise generated by MRI scanners has a tendency to raise stress levels in patients undertaking the scanning. MRI acoustic noise may even lead to temporary or permanent shifts in the hearing threshold for patients [1]. This acoustic noise is mainly caused by the vibration of the gradient coil system due to the Lorentz forces generated by the interaction of the magnetic field around the conductors in the gradient coil and the main static magnetic field. Noise levels as high as 120 –130 dB have been reported in some MRI scanners [2]. The increase in acoustic noise levels in recent years is primarily due to the trend toward the use of high static magnetic field strengths and high-performance switching gradients with high maximum amplitudes and slew rates.

Measures have been taken to control the acoustic noise generated by MRI scanners recently. The technique of Active Noise Control (ANC) for the reduction of MRI noise has been studied by Mechefske *et al.* [3], but it is normally effective at low frequency and less effective at high frequency. Mansfield *et al.*[4] proposed a new technique called active acoustic screening for quiet gradient coil design. Unfortunately, this acoustic screening inevitably reduces the gradient strength. Yoshida *et al.*[5] used "independent suspension" of the coil to dampen solid vibration; while "vacuum vessel enclosure" of the coil shields transmission of residual vibration through the air. However, these methods are not suitable for all kinds of MRI scanners.

It is obvious that optimizing the design of gradient coil systems will eliminate the root cause of the noise. Thus, a good understanding on the characteristics of acoustic radiation of the gradient coil system is necessary for the design of quiet MRI scanners. Due to the geometrical symmetry of the gradient coil system, an analytical model of finite cylindrical ducts with infinite flanges is used to investigate its acoustic radiation characteristics (see Figure 1) in this paper. The radiation impedances will be calculated for a finite cylindrical duct with rigid and absorptive walls. Based on these results, the inside sound field generated by the vibrating wall will be simulated.

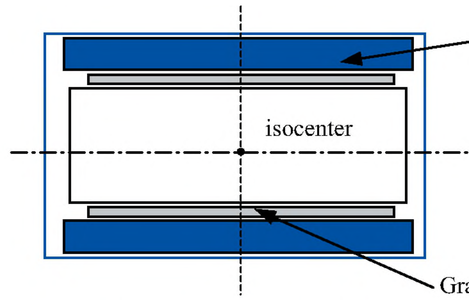

Figure 1. Schematic cross-sectional view of a MRI scanner

2. THEORY

The sound field inside an infinite cylindrical duct can be expressed as a sum of modal solutions (a time factor $e^{i\omega t}$ is understood throughout this paper)

$$p(r,\theta,x) = \sum_{m=-\infty}^{\infty} \sum_{n=1}^{\infty} J_m(\alpha_r^{mn} r) e^{-im\theta} [A_{mn} e^{-i\alpha_x^{mn} x} + B_{mn} e^{i\alpha_x^{mn} x}] \qquad (1)$$

where x is the coordinate in the axial direction of the duct, r is in the radial direction and θ is in the circumferential direction. $J_m(\alpha_r^{mn} r)$ are the Bessel functions of the first kind of circumferential order m, n is the radial mode number. α_x and α_r are the wavenumbers in the axial and the radial direction respectively. A and B are the modal coefficients of the forward-propagating and backward-propagating acoustic wave modes respectively.

For the duct wall with a finite acoustic impedance, the boundary condition should satisfy the equation:

$$\alpha_r^{mn} J'_m(\alpha_r^{mn} a) = i\beta k J_m(\alpha_r^{mn} a) \qquad (2)$$

where a is the radius of the duct and β is a specific acoustic admittance of the wall. The acoustic pressure and velocity amplitudes at the open ends of the duct can be expressed in terms of the acoustic modes in radial r and circumferential θ directions as

$$p(r,\theta,x) = \sum_{m=-\infty}^{\infty} e^{-im\theta} \sum_{n=1}^{\infty} P_{mn} J_m(\alpha_r^{mn} r) \qquad (3)$$

$$u_x(r,\theta,x) = \frac{1}{\rho c}\sum_{m=-\infty}^{\infty} e^{-im\theta}\sum_{n=1}^{\infty} V_{mn} J_m(\alpha_r^{mn} r) \quad (4)$$

where P_{mn} and V_{mn} are the modal coefficients for the pressure and velocity respectively. The relation between the modal pressure and velocity amplitudes can be expressed by the generalized radiation impedance z at the open end:

$$P_{mn} = \sum_{l=1}^{\infty} Z_{mnl} V_{ml} \quad (5)$$

The impedance z can be calculated by the continuity of pressure and velocity at the open ends. The velocity distribution of the vibrating wall can be written in the form of a Fourier series:

$$u_r(a,\theta,x) = \frac{1}{4\pi^2}\sum_{m=-\infty}^{\infty} e^{-im\theta}\int_{-\infty}^{\infty}\tilde{U}_m e^{-i\alpha_x x}\, d\alpha_x \quad (6)$$

Therefore the total sound pressure inside the duct can be calculated by solving the equation (1) by satisfying the boundary conditions at the wall (vibrating and finite impedance) and the open ends (radiation impedance).

3. RESULTS

To verify the validity of the above mathematical model, the sound pressures in the isocenter of a finite cylindrical duct will be calculated. Assuming different wall acoustic impedances: rigid and $\beta = 0.1$, the cylindrical duct with 0.3 m radius and 1.2 m length will be used for the simulations. These results will be compared with the data calculated by the commercial code LMS SYSNOISE, which is based on the Boundary Element Method (BEM).

A uniform velocity distribution with an amplitude 0.0001 *m* is used to move the duct wall. The sound pressures at the isocenter calculated by both the analytical model and BEM model with rigid wall and absorptive wall ($\beta = 0.1$) are shown in Figures 2 and 3 respectively. Comparing these two figures, It can been seen that the overall general shape of all the curves is the same. This suggests good agreement at all frequencies between the BEM results and the analytical results.

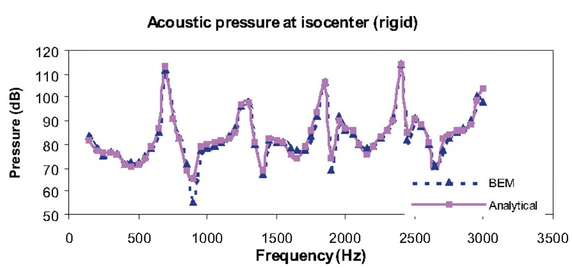

Figure 2. Acoustic pressures at the isocenter (rigid wall)

It can also be seen that an absorptive wall can significantly reduce the noise inside the duct. It is also obvious that there are five peaks in these frequency spectra. This is due to the fact that the wave reflections at the open ends reach their maximum value at the cut-off frequency, therefore causing acoustic resonance. The cut-off frequencies are dependent on the geometrical dimension (radius) of the duct.

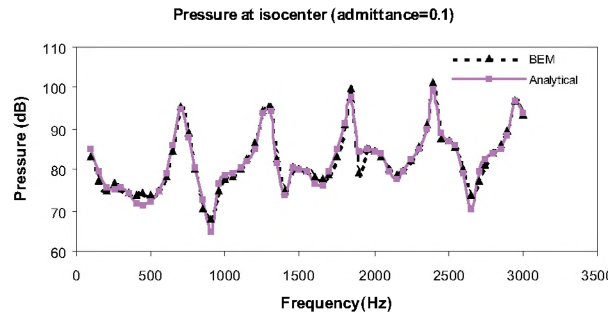

Figure 3. Acoustic pressures at the isocenter ($\beta = 0.1$)

4. CONCLUSIONS

An analytical model that predicts the acoustic noise radiation from gradient coils in MRI scanners has been presented. The acoustic response of the analytical model was found to be in good agreement with the results obtained using a BEM model. Compared with BEM, the most important feature of analytical methods is that they can generally show the dominant parameters for the modeled problems more directly and yield more physical insight. In addition, they are always much more computationally efficient (For instance, it normally takes about 2 weeks for calculating a model with absorptive walls from 100 to 3000 Hz using the BEM in a computer while the same calculation required only two or three hours for the analytical model in the same computer).

REFERENCES:

1. Brumment RE, Talbot GM, Charuhas P. (1988). Potential hearing loss resulting from MR imaging." Radiology, **169**:539-540.
2. Counter SA, Olofsson A, Borg E. (2000). Analysis of magnetic resonance imaging acoustic noise generated by a 4.7 T experimental system. Acta Otolaryngol **120**: 739-743.
3. Mechefske CK and Geris R. (2002). Active noise control for use inside a magnetic resonance imaging machine. Ninth International Congress on Sound and Vibration.
4. Mansfield P, Glover P and Bowtel R, (1994) Active acoustic screening: design principles for quiet gradient coils in MRI. Meas. Sci. Technol. **5**, 1021-1025.
5. Yoshida T, Takamori H and Katsunuma A, (2001) Excelart[TM] MRI system with revolutionary Pianssimo[TM] noise-reduction technology. Med. Rev. **71**,1-4.
6. A. Kuijpers, S. W. Rienstra, G. Verbeek and J. W. Verheij. (1998). The acoustic radiation of baffled finite ducts with vibrating walls. J. Sound Vib. **216**, 461-493.